

Formation and Study of Nanostructured M–Monolayers and LS–Films of Triphenylcorrole

Thao T. Vu,^a Larissa A. Maiorova,^{a@} Dmitrii B. Berezin,^a and Oskar I. Koifman^{a,b}

*Dedicated to Academician of Russian Academy of Sciences Oleg Sinyashin
on the occasion of his birthday*

^aResearch Institute of Macroheterocycles, Ivanovo State University of Chemistry and Technology, 153000 Ivanovo, Russian Federation

^bG.A. Krestov Institute of Solution Chemistry, Russian Academy of Sciences, 153045 Ivanovo, Russian Federation

@Corresponding author E-mail: valkova@mail.ru

An experimental and theoretical study of 5,10,15-triphenylcorrole ($H_3[(ms-Ph)_3Cor]$) nano-structured floating layers (M-layers) was performed. The existence areas and characteristics of the structure and properties of stable monomolecular layers were determined. Main dependencies of the M-monolayer on the initial surface coverage degree were identified – the sizes of the nanoaggregate, aggregation number, surface area per molecule in a nanoaggregate, etc. A quantitative model of a monolayer with water and dry M-nanoaggregates was constructed. $H_3[(ms-Ph)_3Cor]$ thin films on solid substrates were obtained using the Langmuir-Schaefer (LS) technique, and their spectral characteristics were explored.

Keywords: Floating monolayers, 2D nanostructures, M-nanoaggregates, model of M-monolayer, LS-films, corrole.

Формирование и исследование наноструктурированных M–монослоев и ЛШ–пленок трифенилкоррола

Тхао Т. Ву,^a Л. А. Майорова,^{a@} Д. Б. Березин,^a О. И. Койфман^{a,b}

Посвящается академику РАН Олегу Герольдовичу Синяшину по случаю его юбилея

^aНИИ макрогетероциклических соединений, Ивановский государственный химико-технологический университет, 153000 Иваново, Россия

^bИнститут химии растворов им. Г.А. Крестова РАН, 153045 Иваново, Россия

@E-mail: valkova@mail.ru

Выполнено экспериментальное и теоретическое исследование наноструктурированных плавающих слоев (M-слоев) тетрапиррольного макроциклического соединения – 5,10,15-трифенилкоррола ($H_3[(ms-Ph)_3Cor]$). Определены области существования и характеристики структуры и свойств стабильных мономолекулярных слоев. Установлены зависимости основных характеристик M-монослоя – размера наноагрегата, агрегационного числа, площади, приходящейся на молекулу в наноагрегате, и др. от исходной степени покрытия поверхности. Построена количественная модель монослоя с водными и сухими M-наноагрегатами. Методом Ленгмюра-Шефера (ЛШ) получены тонкие пленки $H_3[(ms-Ph)_3Cor]$ на твердых подложках и изучены их спектральные характеристики.

Ключевые слова: Плавающие монослои, 2D наноструктуры, M-наноагрегаты, модель M-монослоя, ЛШ-пленки, коррол.

Introduction

Corroles are tetrapyrrolic macrocyclic porphyrin-like compounds which contain a pyrrole-pyrrole direct coupling and have a carbon skeleton, resembling the B₁₂ vitamin. The peculiarities of the electronic structure of corroles (H₃Ph₃Cor) (Figure 1) and their metal complexes (MCor), morphological variety and unique photophysical and chemical properties have raised interest to them as potential catalyzers for redox processes, chemical sensors for small molecules, and active centers when producing nanomaterials for the area of medicine.^[1,2] When complexes are formed, the corroles, being non-innocent ligands, stabilize metal ions in unusual oxidation degrees, which cause the complexes to suffer slight reversible intramolecular redox transformations.^[3-9] This property accounts for the compounds' high catalytic activity.^[10] One of today's emerging trends is focused on creation of thin-film organic materials, including based on corroles,^[11-20] especially those, where structural and functional units are represented by 2D and 3D nanoparticles.^[21,22] First supermolecules of macroheterocyclic compounds were obtained.^[16-18] Thin films of corroles can be obtained in different ways, including vacuum sublimation, solution casting, and Langmuir-Blodgett techniques (LB). The last one creates ultrathin (as fine as monomolecular) films, which have a desired shape and adjustable structure, with a large specific surface. Such corrole films can be used as potential components for electrode nanomaterials as well.

Properties of thin-film organic nanomaterials are determined by their structure, which depends on the structure of the floating layers when using the LB technique. Studies of Langmuir layers of organic compounds with complex molecular structure have shown, among other things that the compounds' behaviour within the layer depends on the volumetric concentration of the applied solution and the initial surface concentration of the compound under study.^[23-25] A technique to determine quantitative characteristics of a floating layer, the structural and functional units of which are represented by 2D nanoaggregates sized 5-20 nm (*M*-nanoaggregates) was developed and successfully used for describing floating layers of calamite mesogens,^[26] porphyrins,^[27] and phthalocyanines.^[28-30]

The objectives of this study are to: explore features of 5,10,15-triphenylcorrole (H₃[(*ms*-Ph)₃Cor]) floating layer formation under various initial surface coverage degrees; obtain stable *M*-monolayers with various structures of 2D nanoaggregates; determine characteristics of floating monolayers; construct a model of monolayers with water and dry *M*-nanoaggregates; obtain, by using the Langmuir Schaefer (LS) technique as well, H₃[(*ms*-Ph)₃Cor] thin films on solid substrates and study them with UV-Vis spectroscopy.

Experimental

5,10,15-Triphenylcorrole was obtained using a technique, described earlier.^[31,32] Its structure was confirmed by ¹N NMR, IR and UV-Vis spectra. The floating layers were obtained by applying the H₃[(*ms*-Ph)₃Cor] solution in methylene chloride ($C = 6.9 \cdot 10^{-5} \text{ mol} \cdot \text{l}^{-1}$) to the surface of bi-distilled water with

microliter syringes (1, 10, 20, and 100 μl, "Hamilton", Sweden) at the temperature of $20 \pm 1 \text{ }^\circ\text{C}$. The layers were compressed at the speed of $2.3 \text{ cm}^2 \cdot \text{min}^{-1}$ 15 minutes after the solution had been applied to the water surface. Initial degrees of water surface coverage with corrole (C_{face}) changed from 4 % to 29 %. An "NT (MDT" unit (Zelenograd, Russia) was used for the experiment. The surface pressure was measured by using a Wilhelmy plate with an accuracy of $0.02 \text{ mN} \cdot \text{m}^{-1}$. Error of measurement with respect to a surface area per molecule in the layer (A) was 2 %. A_{mol} values (surface area per molecule in an *M*-aggregate) and n (aggregation number) were determined by approximation of πA - π curve's portion with a linear function, by using the least squares technique (error $\pi A \leq 3 \%$). The Langmuir-Schaeffer (LS) films were obtained by transferring the floating layer to the quartz plate under conditions, shown on Figure 3 (point A). Electronic absorption spectra were registered on a UV/VIS Lambda 20 scanning spectrophotometer with $\pm 0.1 \text{ nm}$ wavelength setting accuracy. The reproducibility of the wavelength setting was $\pm 0.05 \text{ nm}$, the photometric accuracy being ± 0.003 . The structure of the layers was analyzed by using quantitative analysis of compression isotherms of a nanostructured *M*-monolayer.^[33-35] The main characteristics of the floating layer were determined in the following manner: $\beta = kT/n$, where β is the ordinate of the intersection point between the line, describing the isotherm's πA - π region corresponding to the stable state of the layer, and the πA axis; A_{mol} is the line's tilt. According to the model being used, *M*-aggregate has a shape of a circle with the surface area of $S_{\text{aggr}} = A_{\text{mol}} \cdot n \text{ (nm}^2\text{)}$ and the diameter of $D_{\text{aggr}} = \sqrt{4S_{\text{aggr}}/\pi} \text{ (nm)}$. The layer's compressibility in a stable state can be defined as

$$B = \frac{A_i - A_f}{(\pi_f - \pi_i) \cdot A_i} \text{ (m/N)}, \text{ where } \pi_i \text{ and } \pi_f \text{ are the respective pressures}$$

at the start and at the end of the monolayer's stable state, with A_i and A_f being the abscissas of the start and the end of the linear portion of the πA -isotherm. The distance between the boundaries of the aggregates is the same on the average, and can be calculated from the relation:

$$d_i = \sqrt{\frac{A_i \cdot n}{\pi}} - \sqrt{\frac{4A_{\text{mol}} \cdot n}{\pi}} \text{ (nm)}. \text{ The average distance between}$$

the molecules along the surface of the water (*face-on*) in an M_{face} -

aggregate will be $r = \sqrt{\frac{4A_{\text{mol}}}{\pi}} - \sqrt{\frac{4A_{\text{proj}}}{\pi}} \text{ (nm)}$. Water coverage

degrees at the initial point of the stable state can be defined as $c_{i\text{-face}} = A_{\text{proj-face}}/A_i \cdot 100\%$ and $c_{i\text{-edge}} = A_{\text{proj-edge}}/A_i \cdot 100\%$, where $A_{\text{proj-face}}$ and $A_{\text{proj-edge}}$ are surface areas of *face-on* and *edge-on* projections of molecule models. Within the linear portion on curve πA - π , the tilt of the molecules (which have an anisotropic shape) in the stack of a compact nonaqueous aggregate can be defined as $\psi = \arcsin(A_{\text{pack-edge}}/A_{\text{mol}})$, where $A_{\text{pack-edge}}$ is the closest packed surface area. The content of water in *M*-aggregates (calculated per molecule) and between them at the initial point of the stable state can be calculated with $w_{\text{in-M}} = A_{\text{mol}} - A_{\text{proj}}$ and $w_{\text{inter-M-i}} = A_i - A_{\text{mol}}$ expressions respectively.

Geometric characteristics of the molecules and their closest packings were determined by constructing the corresponding molecular models (HyperChem 8.0.8, MM+ calculations). The surface areas of projections in case of *face-on* and *edge-on* positions of the molecules were found to be: $A_{\text{proj(face)}} = 1.6 \text{ nm}^2$, $A_{\text{proj-1(edge)}} = 0.8 \text{ nm}^2$, $A_{\text{proj-2(edge)}} = 1.0 \text{ nm}^2$; with the surface areas of the described rectangles being $A_{\text{mod(face)}} = 3.2 \text{ nm}^2$ and $A_{\text{mod-1(edge)}} = 1.1 \text{ nm}^2$, $A_{\text{mod-2(edge)}} = 1.4 \text{ nm}^2$, respectively (Figure 1).

Surface areas, occupied by a molecule in a closest packed monolayer will be $A_{\text{pack(face)}} = 1.9 \text{ nm}^2$, $A_{\text{pack(edge-1)}} = 1.0 \text{ nm}^2$ and $A_{\text{pack(edge-2)}} = 1.2 \text{ nm}^2$ (Figure 2). The maximum error when defining characteristics of a layer is: A_{mol} and $D\pi - 3 \%$, c_{face} and $y - 5 \%$, D and $w_{\text{inter-M-i}} - 7 \%$, B , $c_{i\text{-face}}$, c_{face} , $c_{i\text{-edge}}$, c_{edge} , n , $w_{\text{in-M}}$ and $d_i - 10 \%$.

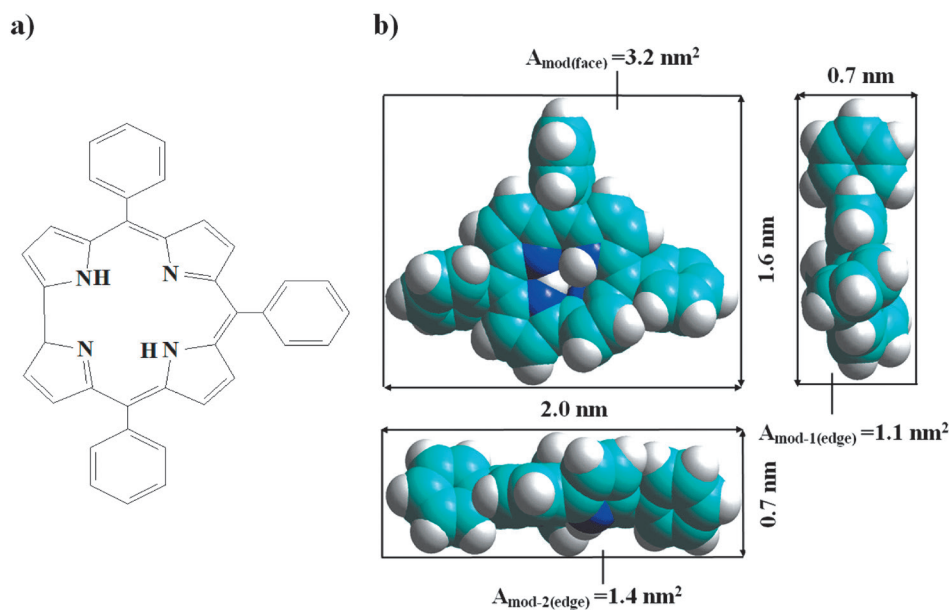


Figure 1. Structure (a) and model of H_3Ph_3Cor molecule (b). A_{mod} – the surface areas of circumscribed rectangles.

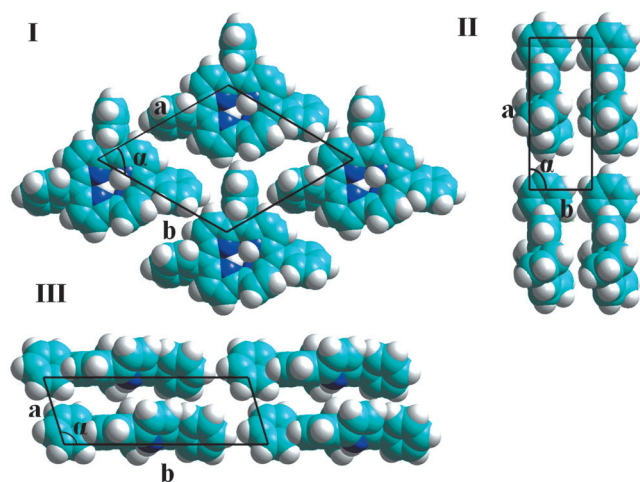


Figure 2. The scheme of *face-on* (I) and *edge-on* (II, III) closest packed molecules of $H_3[(ms-Ph)_3Cor]$.
 $A_{pack(face)} = 1.9 \text{ nm}^2$ ($a = 1.5 \text{ nm}$; $b = 1.5 \text{ nm}$; $\alpha = 60^\circ$, I),
 $A_{pack(edge_1)} = 1.0 \text{ nm}^2$ ($a = 1.6 \text{ nm}$; $b = 0.6 \text{ nm}$; $\alpha = 86^\circ$, II),
 $A_{pack(edge_2)} = 1.2 \text{ nm}^2$ ($a = 0.6 \text{ nm}$; $b = 2.0 \text{ nm}$; $\alpha = 108^\circ$, III).

Results and Discussion

The quantitative analysis of compression isotherms plotted along π - A and πA - π axes (Figure 3) has shown that both stable monolayers and bilayers $H_3[(ms-Ph)_3Cor]$ are formed on the water surface within the studied in 4–29 % range of initial coverage degrees (c_{face}). The main results of compression isotherm analysis and characteristics of $H_3[(ms-Ph)_3Cor]$ floating layers are shown in Table 1. It is demonstrated that a corrole given the $C = 6.9 \cdot 10^{-5} \text{ mol} \cdot \text{l}^{-1}$ concentration of the solution and the $v = 2.3 \text{ cm}^2/\text{min}$ layer compression speed forms stable monolayers in a narrow range of initial surface coverage degrees – c_{face} from 4 % to 22.5 % (Figure 3). If the values are $c_{face} > 22.5 \%$, bilayers

are registered already at the lowest surface pressures. Corroles produce stable monolayers of different types: if $c_{face} \leq 13.5 \%$, they have the *face-on* position of molecules in nanoaggregates (M_{face}), if $19.5 \% \geq c_{face} \geq 13.9 \%$, they have the *edge-on* position (M_{edge}), and if $c_{face} = 20 \%$, then dry nanoaggregates (M_n) are formed.

Monolayers with *face-on* position are characterized by a large aggregation number ($13 < n < 81$) (Table 1) and a high content of water in aquaaggregates (up to 70 % of A_{mol}) and between them (up to 1.6 nm^2 per H_3Ph_3Cor molecule). A monolayer has high compressibility (up to $750 \text{ m} \cdot \text{N}^{-1}$). If values of initial surface coverage degrees ($19.5 \% \geq c_{face} \geq 13.9 \%$) are average, the low pressure regions form stable *edge-on*-monolayers, where the molecule's plane is positioned at an angle to the water surface. The minimum tilt (ψ_{min}) of H_3Ph_3Cor molecules in stacks varies from 38° to 60° , with the number of molecules in M_{edge} -aggregates varying from 29 to 67, the content of water between aggregates varying from 0.4 to 0.9 nm^2 per molecule, and the layer compressibility being low (down to $430 \text{ m} \cdot \text{N}^{-1}$). A monolayer of dry *edge-on* M_c -aggregates is characterized by low layer compressibility, $B = 380 \text{ m} \cdot \text{N}^{-1}$, the minimum number of molecules in aggregates ($n = 17$) and the maximum content of water between aggregates at the initial point of the stable monolayer state ($w_{inter-M-i} = 2.5 \text{ nm}^2$). If the initial surface coverage degrees are high ($c_{face} = 23.2 \%$), the surface pressure of up to 0.4 mN/m forms a stable bilayer structure (3D-nanoaggregates with 79–151 molecules in them).

The obtained results can be used to construct a model of H_3Ph_3Cor M_{face} - and M_{edge} -floating monolayers formed from the solution in methylene chloride. For monolayers with M_{face} - and M_{edge} -aggregates the analysis of dependencies of the surface area per nanoaggregate molecule on the initial surface coverage degree (Table 1, Figure 4a) results in the following correlations:

$$A_{mol} = 26 / (1 + c_{face}) \quad (\text{for } M_{face} \text{ - aquaaggregates}) \quad (1)$$

$$A_{mol} = 4.067 - 0.162 \cdot c_{face} \quad (\text{for } M_{edge} \text{ - aquaaggregates}) \quad (2)$$

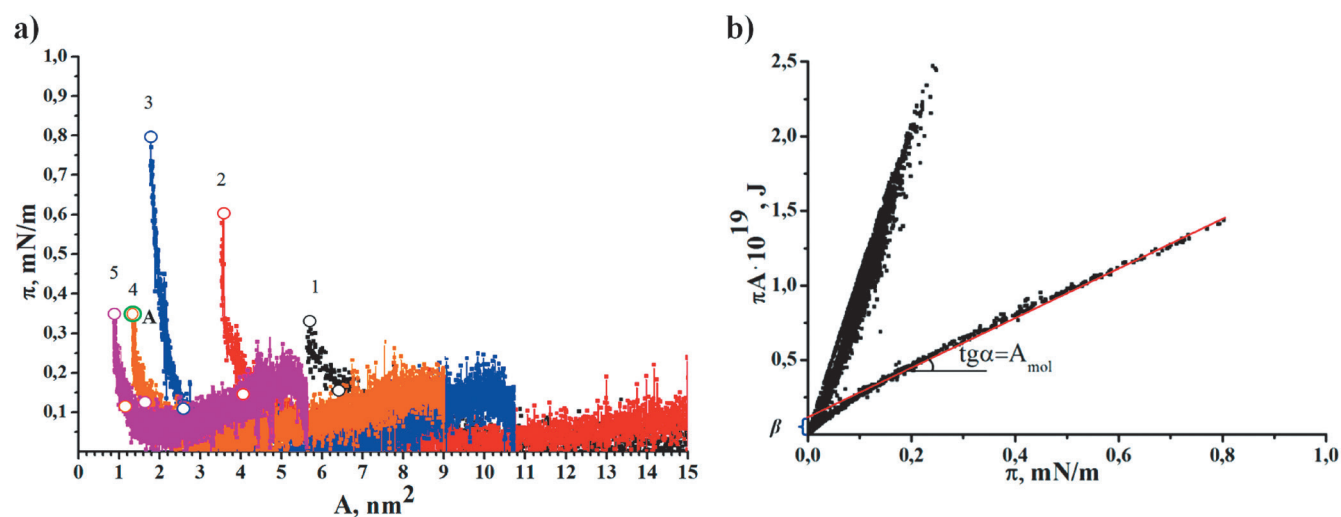


Figure 3. π - A (a) isotherms of $H_3[(ms-Ph)_3Cor]$, obtained at $C=6.9 \cdot 10^{-5}$ mol/l, $v=2.3$ cm²/min and various initial surface coverage degrees: $c_{face} = 4(1), 7(2), 15(3), 18(4), 29(5)$ % and πA - π (b) isotherm of $H_3[(ms-Ph)_3Cor]$ ($c_{face} = 15$ %). The floating *M*-monolayer was transferred onto a solid support by dips at $\pi_{tr}=0.35$ mN/m (point A on Figure 3a).

Table 1. Characteristics of $H_3[(ms-Ph)_3Cor]$ floating layers, obtained at different initial surface coverage degrees.

c_{face} (%)	Nanoaggregate-type	c_{i-face} - c_{f-face} (Δc_{i-face}) (%)	c_{i-aggr} (%)	$(\Delta\pi)$ $\pi_i - \pi_f$ (mN/m)	A_{mol} (nm ²)	n	D_{aggr} (S_{aggr}) (nm) (nm ²)	Ψ_{min} - Ψ_{max} (°)	r (nm)	w_{in-M}/A_{mol} (%)	$w_{inter-M-i}$ (nm ²)	d_i (nm)	B (m/N)
$H_3Ph_3Cor = 6.9 \cdot 10^{-5}$ mol · l ⁻¹ (layer compression speed $v=2.3$ cm ² /min.)													
4	M_{face}	24-28 (4)	76	0.1-0.3	5.2	13	9 (70)	0	1.1	69	1.6	1.3	750
7	M_{face}	34-45 (11)	69	0.1-0.6	3.3	31	11 (100)	0	0.6	52	1.5	2.3	540
8	M_{face}	43-58 (15)	70	0.1-0.6	2.6	45	12 (120)	0	0.4	38	1.1	2.3	500
10	M_{face}	55-67 (12)	77	0.1-0.5	2.3	58	13 (130)	0	0.3	29	0.7	1.7	500
13	M_{face}	62-81 (19)	74	0.1-0.6	1.9	81	14 (150)	0	0.1	16	0.6	2.3	450
15	M_{edge}	32-45 (13)	66	0.1-0.8	1.6	29	8 (50)	38°-90	-	51	0.9	1.8	430
17	M_{edge}	41-50 (9)	67	0.1-0.5	1.3	49	9 (60)	50°-90	-	38	0.6	2.0	430
18	M_{edge}	52-58 (6)	75	0.1-0.4	1.2	67	10 (80)	60°-90	-	31	0.4	1.5	410
20	$M\chi$	40-79 (7)	83	0.1-1.4	1.1	17	5 (20)	90	-	0	0.4	2.5	380
25	<i>bilayer</i>	-	-	0.2-0.4	0.8	79	-	-	-	-	-	1.8	670
29	<i>bilayer</i>	-	-	0.2-0.4	0.8	151	-	-	-	-	-	1.8	550

c_{face} initial surface coverage degree; c_{i-face} and c_{f-face} current surface coverage degrees at the initial and final points of the stable state, respectively; Δc_{i-face} state existence region with respect to the current surface coverage degree; c_{i-aggr} the degree of surface coverage with *M*-aggregates at the initial point of the stable state; $\pi_i - \pi_f$ ($\Delta\pi$) pressure region, in which the stable state exists; A_{mol} surface area per molecule in a nanoaggregate; n aggregation number; D_{aggr} and S_{aggr} the diameter and surface area of a nanoaggregate; Ψ_{min} the minimum tilt of molecules in stacks ("dry" aggregates); w_{in-M} and $w_{inter-M-i}$ the content of water in *M*-aggregates and between them (per molecule) at the initial point of the stable state; r the average distance between molecule in an aggregate; d_i, d_f the distance between nanoaggregates at the initial and final points of the stable state; B compressibility of the layer.

*The values of $A_{proj-1(edge)} = 0.8$ nm², $A_{pak-1(edge)} = 1.0$ nm² were used in calculations.

They can help to determine constants, characterizing the H_3Ph_3Cor floating layer: the maximum surface area per molecule in an *edge-on*-monolayer (1.8 nm^2), and the maximum initial surface coverage values causing such *face-on*- and *edge-on* monolayers to be formed: $c_{face} = 13.5 \%$ and $c_{face} = 19.5 \%$, respectively. Analysis of dependence on the initial surface coverage degree with respect to other characteristics of a monolayer (Table 1, Figure 4b-d) resulted in the following correlations.

For M_{face} monolayers:

$$n = -24.8 + 8.1 \cdot c_{face} \quad (3)$$

$$D_{aggr} = 7.7 + 0.5 \cdot c_{face} \quad (4)$$

$$w_{in-M}/A_{mol} = 93.7 - 6.2 \cdot c_{face} \quad (5)$$

$$c_{i-face} = 4.7 + 4.6 \cdot c_{face} \quad (6)$$

$$c_{f-face} = 4.8 + 6.0 \cdot c_{face} \quad (7)$$

and for M_{edge} monolayers:

$$n = -164.3 + 12.9 \cdot c_{face} \quad (8)$$

$$D_{aggr} = -3.2 + 0.7 \cdot c_{face} \quad (9)$$

$$w_{in-M}/A_{mol} = 150.5 - 6.6 \cdot c_{face} \quad (10)$$

$$c_{i-face} = -66.4 + 6.5 \cdot c_{face} \quad (11)$$

$$c_{f-face} = -19.7 + 4.3 \cdot c_{face} \quad (12)$$

The results obtained make it possible to compile a passport^[35] of the floating layers of H_3Ph_3Cor (Table 2). The schemes illustrating the fragment and main structural characteristics of monolayers with *face-on* ($c_{face} = 4 \%$)

and *edge-on* aquaaggregates ($c_{face} = 15 \%$), and with dry nanoaggregates ($c_{face} = 20 \%$) are shown in Figure 5.

LS-films of H_3Ph_3Cor were formed from the floating monolayer produced on the water surface by using the horizontal lift method. Figure 6 shows UV-Vis spectra of H_3Ph_3Cor solution in methylene chloride ($C = 6.9 \cdot 10^{-5} \text{ mol} \cdot \text{l}^{-1}$) and those of LS-films on a quartz substrate. The number of the substrate's immersions (k) into the layer is from 1 to 77. The comparison of the spectra shows a different degree of H_3Ph_3Cor aggregation in the solution and the films. The Soret band of the spectrum of Langmuir-Schaefer films ($\lambda = 421 \text{ nm}$) has a 6 nm red shift relative to the band in the spectrum of the solution ($\lambda = 415 \text{ nm}$). Such behaviour corresponds to formation of *J*-aggregates of corroles in the films.

Conclusions

Thus, the study shows the possibility of differently structured H_3Ph_3Cor floating layers to be formed on a water surface: monolayers with M_{face} -aquaaggregates ($c_{face} \leq 13.5 \%$), M_{edge} -aquaaggregates ($13.9 \% \leq c_{face} \leq 19.5 \%$) and M_{edge} -dry aggregates ($20.0 \% \leq c_{face} \leq 22.5 \%$) and polylayers with 3D nanoaggregates ($c_{face} \geq 23.2 \%$). Main characteristics of the structure and the properties of *M*-monolayers were determined (the size of *M*-nanoaggregates, formed within a layer, the number of molecules in them, the distance between the

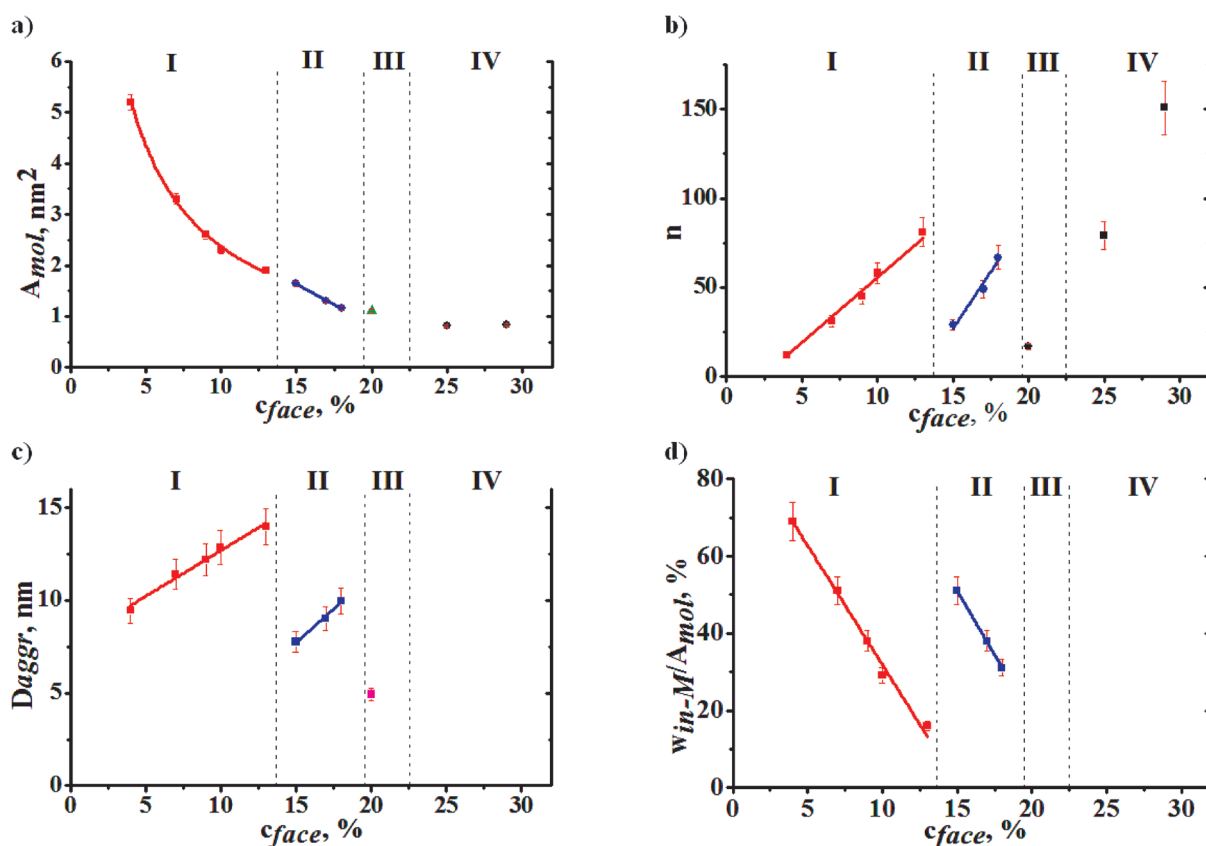


Figure 4. Dependencies of the surface area per molecule in *M*-aggregate (A_{mol} , a), the aggregation number (n , b), the diameter of *M*-nanoaggregates (D_{aggr} , c) and the content of water in nanoaggregates (w_{in-M}/A_{mol} , d) on the initial surface coverage degree. I – monolayers (*face-on*); II – monolayers (*edge-on*); III – monolayers (*edge-dry*); IV – bilayers.

Table 2. Passport of the floating layers of H₃Ph₃Cor.

Nanoaggregate type	Molecular orientation in <i>M</i> -aggregate	Formation conditions (from the model)	Dependences of characteristics of a monolayer on c_{face} (model)	Constants
$C = 6.9 \cdot 10^{-5} \text{ mol} \cdot \text{l}^{-1}$; $v = 2.3 \text{ cm}^2 \cdot \text{min}^{-1}$; $t = 20 \pm 1 \text{ }^\circ\text{C}$				
2D, $M_{face-aqua}$	<i>face-on</i> (<i>in-plane</i>)	$c_{face} \leq 13.5 \%$	$n = -24.8 + 8.1 \cdot c_{face}$ $D_{aggr} = 7.7 + 0.5 \cdot c_{face}$ $w_{in-M}/A_{mol} = 93.7 - 6.2 \cdot c_{face}$ $c_{i-face} = 4.7 + 4.6 \cdot c_{face}$ $c_{f-face} = 4.8 + 6.0 \cdot c_{face}$	$n^{max} = 85$ $(D_{aggr})^{max} = 14.5 \text{ nm}$ $w_{in-M}/A_{mol}^{min} = 10 \%$ $c_{i-aggr} = \text{const} = 73 \%$ $(c_{i-face})^{max} = 67 \%$ $(c_{f-face})^{max} = 86 \%$
2D, $M_{edge-aqua}$	<i>edge-on</i>	$13.9 \leq c_{face} \leq 19.5 \%$	$n = -164.3 + 12.9 \cdot c_{face}$ $D_{aggr} = -3.2 + 0.7 \cdot c_{face}$ $w_{in-M}/A_{mol} = 162.4 - 8.2 \cdot c_{face}$ $c_{i-face} = 66.4 + 6.5 \cdot c_{face}$ $c_{f-face} = -19.7 + 4.3 \cdot c_{face}$	$n^{min} = 15$; $n^{max} = 87$ $(D_{aggr})^{min} = 6.5 \text{ nm}$; $(D_{aggr})^{max} = 10.5 \text{ nm}$ $(w_{in-M}/A_{mol})^{min} = 22 \%$; $(w_{in-M}/A_{mol})^{max} = 48 \%$ $c_{i-aggr} = \text{const} = 69 \%$ $(c_{i-face})^{min} = 24 \%$; $(c_{i-face})^{max} = 60 \%$ $(c_{f-face})^{min} = 40 \%$; $(c_{f-face})^{max} = 64 \%$
2D, dry, M_c	<i>edge-on</i>	$20.0 \leq c_{face} \leq 22.5 \%$		
3D	-	$c_{face} \geq 23.2 \%$		

aggregates, the content of water in the aggregates and between them, compressibility, the existence region with respect to the pressure and the running surface concentration). Dependencies of the main parameters of monolayers with M_{face} and M_{edge} -aggregates on the initial surface coverage degree were determined. A quantitative model of H₃Ph₃Cor monolayers, formed from a solution in methylene chloride, was constructed. A distinctive feature of triphenylcorrole floating *face-on* monolayers is the formation of the dry *M*-nanoaggregates. Conditions for 3D nanoaggregate formation in H₃Ph₃Cor floating layers and the number of molecules in

them were determined. The results obtained make it possible to compile a passport of the floating layers of H₃Ph₃Cor. Langmuir-Shaeffer films were formed from a stable floating monolayer, produced on a water surface. Comparison of the spectra of the solution and the films indicates the formation of *J*-aggregates of H₃Ph₃Cor in films.

Acknowledgements. This work was partially supported by the Russian Foundation for Basic Research (Project N 15-42-03211a) and Ministry of Education and Science of Russian Federation (State task for ISUCT).

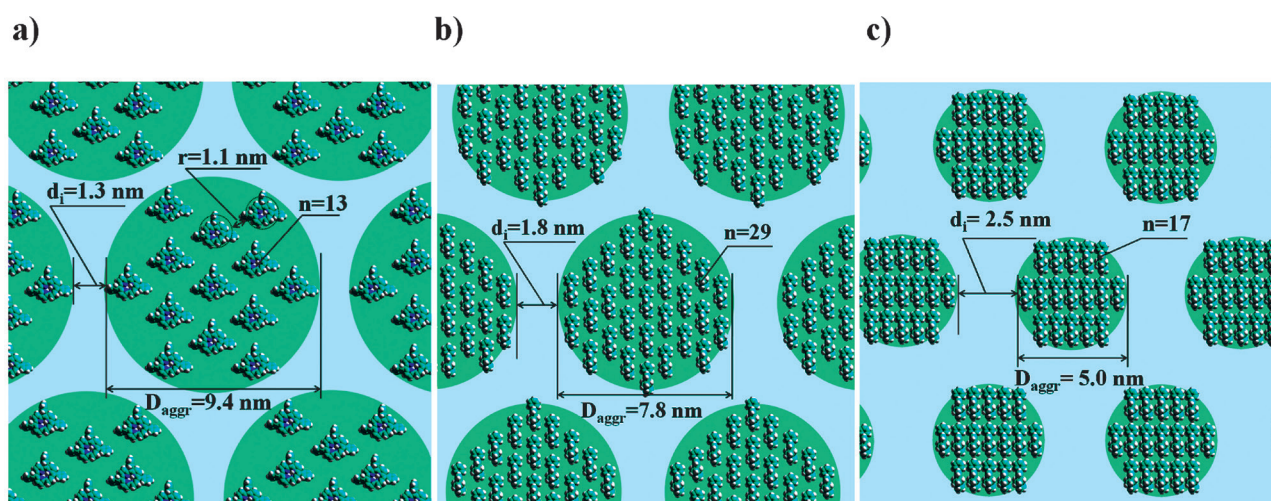


Figure 5. Schemes, illustrating fragments of the structure and main structural characteristics of triphenylcorrole monolayers with *face-on* (a, $c_{face} = 4 \%$) and *edge-on* (b, $c_{face} = 15 \%$) aquaaggregates, and also dry *edge-on* (c, $c_{face} = 20 \%$) nanoaggregates.

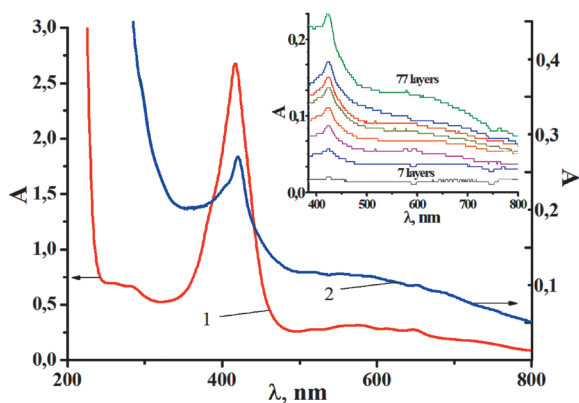


Figure 6. Absorption spectra of the H_3Ph_3Cor ($C=3.6 \cdot 10^{-5}$ mol/l) solution in CH_2Cl_2 (1) and its Langmuir-Schaefer films (77 edge-on monolayers, 2). Inset: absorption spectra of LS-films (7, 28, 35, 42, 49, 63, 70 and 77 edge-on monolayers).

References

- Aviv I., Gross Z. *Chem. Commun.* **2007**, 1987-1999.
- Hwang J.Y., Lubow J., Chu D., Ma J., Agadjanian H., Sims J., Gray H.B., Gross Z., Farkas D.L., Medina-Kauwe L.K. *Mol. Pharm.* **2011**, *8*, 2233–2243.
- Berezina N.M., Vu T.T., Karimov D.R., Kumeev R.S., Kustov A.V., Bazanov M.I., Berezin D.B. *Russ. J. Gen. Chem.* **2014**, *84*, 737–744.
- Liua H.-Y., Mahmooda M.H., Qiuc S.-X., Chang C.K. *Coord. Chem. Rev.* **2013**, *257*, 1306–1333.
- Thomas K., Alemayehu A.B., Conradie J., Beavers C.M., Ghosh A. *Acc. Chem. Res.* **2012**, *45*, 1203–1214.
- Aviv-Harel I., Gross Z. *Coord. Chem. Rev.* **2011**, *255*, 717–736.
- Paolo S., Anna A., Mariachiara P., Giuseppe V., Kolanu S.L.G., Yarasi S., Filippo D.A. *Computat. Theoret. Chem.* **2014**, *1030*, 59–66.
- Koifman O.I., Nikitina G.E., Berezin B.D. *Zh. Fiz. Khim.* **1982**, *56*, 737 (in Russ.).
- Ivanova Y.B., Savva V.A., Mamardashvili N.Z., Starukhin A.S., Ngo T.H., Dehaen W., Maes W., Kruk M.M. *J. Phys. Chem. A* **2012**, *116*, 10683.
- Zou H., Wang H., Mei G., Liu H., Chang C-K. *Prog. Chem.* **2015**, *27*, 666-674.
- Valkova L.A., Betrencourt C., Hochapfel A., Myagkov I.V., Feigin L.A. *Mol. Cryst. Liq. Cryst.* **1996**, *287*, 269.
- Valkova L., Borovkov N., Koifman O., Kutepov A., Berzina T., Fontana M., Rella R., Valli L. *Biosensors Bioelectronics* **2004**, *20*, 1177.
- Valkova L., Borovkov N., Maccioni E. *et al. Colloids Surf., A* **2002**, *198–200*, 891.
- Paolesse R., Di Natale C., Macagnano A., Sagone F., Scarselli M.A., Chiaradia P., Troitsky V.I., Berzina T.S., D'Amico A. *Langmuir* **1999**, *15*, 1268-1274.
- Bursa B., Wróbel D., Lewandowska K., Graja A., Grzybowski M., Gryko D.T. *Synthetic Metals* **2013**, *176*, 18–25.
- Valkova L., Borovkov N., Kopranenkov V., Pisani M., Bossi M., Rustichelli F. *Mater. Sci. Eng., C* **2002**, *22*, 167.
- Valkova L., Borovkov N., Pisani M., Rustichelli F. *Thin Solid Films* **2001**, *401*, 267.
- Valkova L.A., Valli L., Casilli S., *et al. Langmuir* **2008**, *24*, 4857-4864.
- Tebi S., Aldahhak H., Serrano G., Schöfberger W., Rauls E., Schmidt W.G., Koch R., Müllegger S. *Nanotechnology* **2016**, *27*, 025704.
- Sinha W., Kumar M., Garai A., Purohit C.S., Som T., Kar S. *Dalton Trans.* **2014**, *43*, 12564.
- Maiorova L.A. *Synopsis of D.Sc. (Phys-Math.) Thesis*, Ivanovo, **2012**. 32 p. (in Russ.).
- Valkova L., Menelle A., Borovkov N., *et al. J. Appl. Crystallogr.* **2003**, *36*, 758.
- Valkova L., Borovkov N., Pisani M., Rustichelli F. *Langmuir* **2001**, *17*, 3639.
- Valkova L.A., Shabyshev L.S., Borovkov N.Y., Feigin L.A., Rustichelli F. *J. Inclusion Phenom. Macrocyclic Chem.* **1999**, *35*, 243.
- Valkova L.A., Shabyshev L.S., Feigin L.A., Akopova O.B. *Molecular Materials* **1996**, *6*, 291.
- Maiorova-Valkova L.A., Koifman O.I., Burmistrov V.A. *et al. Protec. Metals Phys. Chem. Surf.* **2015**, *51*, 85.
- Karlyuk M.V., Krygin Y.Y., Maiorova-Valkova L.A., Ageeva T.A., Koifman O.I. *Russ. Chem. Bull.* **2013**, *62*, 471.
- Valkova L.A., Glibin A.S., Koifman O.I. *Macroheterocycles* **2011**, *4*, 3, 222-226.
- Valkova L.A., Glibin A.S., Koifman O.I., Erokhin V.V. *J. Porphyrins Phthalocyanines* **2011**, *15*, 1044.
- Petrova M.V., Maiorova L.A., Gromova O.A., Bulkina T.A., Ageeva T.A., Koifman O.I. *Macroheterocycles* **2014**, *7*, 267.
- Semeikin A.S., Koifman O.I., Berezin B.D. *Chem. Heterocycl. Compd.* **1986**, *22*, 629.
- Zelentsov V.V., Stroesku A.K., Koroleva T.A., Koifman O.I. *Koord. Khim.* **1983**, *9*, 168 (in Russ.).
- Valkova L.A., Glibin A.S., Valli L. *Colloid J.* **2008**, *70*, 6.
- Valkova L., Zyablov S., Erokhin V., Koifman O. *J. Porphyrins Phthalocyanines* **2010**, *14*, 513.
- Maiorova L.A. *D.Sc. (Phys-Math.) Thesis*, Ivanovo, **2012**. 382 p. (in Russ.).

Received 05.12.2015

Accepted 14.02.2016